SELF-OSCILLATING GaAs FET DEMODULATOR AND DOWNCONVERTER FOR MICROWAVE MODULATED OPTICAL SIGNALS

Christen Rauscher†, Lew Goldberg, and Aileen M. Yurek

Naval Research Laboratory
Washington, D.C. 20375

Abstract — Recovery of a high-frequency modulation signal from an optical carrier is accomplished by employing a commercially available single-gate GaAs FET in a multifunctional role. The transistor serves simultaneously as detector, tunable local oscillator, harmonic generator, and mixing element, thereby achieving demodulation and downconversion all in one. Implementation of the concept is illustrated with an experimental circuit that uses a device with sub-quarter-micron gate geometry and provides an output response in the designated 3-to-7-GHz intermediate-frequency interval. Circuit characteristics are reported for various frequency ranges of optical carrier modulation, demonstrating practicability of the approach up through 90 GHz.

INTRODUCTION

Supported by recent advances in techniques for generating high-speed modulated optical carriers, research interests are being focused on their application to broadband microwave signal transmission. Generating techniques encompass direct modulation of semiconductor laser diodes [1][2], as well as indirect approaches. An example in the latter category is the use of FM sideband injection locking [3], with obtainable modulation frequencies approaching the millimeter-wave regime. On the receiving end, demodulation at these frequencies is also readily achievable. Photodiode-based concepts have been reported [4] in which an individual diode not only serves as a simple detector, but in which diode nonlinearities are simultaneously exploited to produce harmonics of an injected local oscillator signal. The harmonics then mix with the detected modulation signal to produce a downconverted response.

The present study focuses on employing a commercially available single-gate GaAs FET to perform not only the three functions of detection, harmonic generation, and mixing, but to internally generate, in addition, the local oscillator signal needed for the downconversion process. The approach thereby makes comprehensive use of the transistor's sensitivity to optical illumination, its high-frequency active characteristics, and its nonlinear properties.

BASIC CONCEPT

The sensitivity of device characteristics to optical illumination is of course fundamental to the overall approach. The impact of constant-intensity illumination on device performance at microwave frequencies, in particular, is documented in the literature [5]. Similar relationships are assumed to apply for illumination of time-varying intensity. The underlying signal interaction is based on generation of electron-hole pairs within the transistor. Observed effects will depend on where within the device the carriers are generated and on the time constants associated with their velocities and recombination rates. The dominant effects encountered in high-speed applications have been mainly attributed to photoconductive modulation of carrier concentrations in the channel [6]. Regardless of the combination of effects that actually might be involved, it may be generally assumed that both the channel and the depletion region under the gate will be affected by illumination. In terms of a circuit-type device model [7], this would indicate that not only device transconductance and resistive elements, but also gate-source and drain-gate capacitances should be considered dependent on light intensity.

In order to simplify the following discussion, the drain-source current $i_{ds}(t)$ and the current $i_{cg}(t)$ through the main gate-source capacitance will be singled out to represent all dependent effects influencing transistor behavior. For simplicity, the current values shall depend only on the gate-source voltage and the absorbed optical power, according to the truncated phenomenological relationships

$$i_{ds}(t) = I_{ds} + g_{v1} \cdot v_{gs}(t) + g_{v2} \cdot v_{gs}^2(t) + g_{o1} \cdot p_{opt}(t) + g_{vo} \cdot v_{gs}(t) \cdot p_{opt}(t) + \ldots \quad (1)$$

and

$$i_{cg}(t) = c_{v1} \cdot \frac{dv_{gs}(t)}{dt} + c_{v2} \cdot v_{gs} \cdot \frac{dv_{gs}(t)}{dt} + c_{vo} \cdot \frac{d}{dt}\{v_{gs}(t) \cdot p_{opt}(t)\} + \ldots \quad (2)$$

The quantities $v_{gs}(t)$ and $p_{opt}(t)$ refer to the *time-varying* components of the gate-source voltage and optical power, respectively, with the various g- and c-factors denoting constant coefficients. The second expression assumes that the gate-source capacitance may be approximated by a linearized dependence of its value on the two time-varying parameters. Higher-order terms in $p_{opt}(t)$ are ignored, as the optical signal is assumed to be small-signal in nature.

The above relationships serve to qualitatively describe the multifunction task assigned to the transistor. Device gain is symbolically represented by the linear term in $v_{gs}(t)$ in

†Currently on sabbatical leave at the Los Alamos National Laboratory, Los Alamos, NM 87545.

0149-645X/86/0000-0721$01.00 © 1986 IEEE

expression (1), supplying the basis for sustaining local oscillation at a predetermined frequency within the active frequency range of the transistor. Harmonics of the local oscillator signal are generated with the help of device nonlinearities. Second harmonic generation, in particular, is associated with the quadratic terms in the two expressions. The transconductance-related term will normally dominate, especially when the transistor is biased in the vicinity of pinch-off [8]. As for the recovery of the high-frequency modulation signal from the optical carrier, this is partially accounted for by the linear term $g_{o1} \cdot p_{opt}(t)$ which, in turn, is representative of first-order photoconductive effects on transistor characteristics. A portion of the detected modulation signal gets fed back to the transistor input via the device-external circuit and the device-internal parasitics. This signal then mixes with the local oscillator signal and its harmonics. The mixing process thereby relies on the quadratic transconductance nonlinearity already employed in the generation of the local oscillator harmonics. A filter is used to select the desired difference-frequency signal among the various signal products.

In addition to the composite demodulation and downconversion process just described, the two mixed-product terms in the phenomenological expressions postulate an alternate and direct mechanism for transposition of the optical carrier modulation signal to the designated intermediate-frequency band. The mixed-product term in expression (1) allows for operation analogous to that of a dual-gate FET, except that here one of the signals subjected to multiplication is injected optically, whereas the corresponding term in expression (2) provides for possible parametric effects. The whole demodulation and downconversion process is thus a composition of various phenomena alluded to here and in the previous paragraph. The relative significance of individual contributions, and the manner in which they interact with each other, are functions of intrinsic device characteristics, as well as functions of device-external bias and circuit conditions.

PHYSICAL IMPLEMENTATION

The experimental circuit, which has been employed in the testing of the overall concept, is shown in Fig. 1. Its physical realization is in microstrip, implemented on a 0.25-mm-thick fiberglass-reinforced Teflon substrate. The corresponding schematic circuit diagram is given in Fig. 2. The circuit comprises a front-end section, responsible for performing the multiple tasks discussed in the preceding section, followed by an intermediate-frequency gain stage. The two basic segments of the circuit are readily distinguishable in Fig. 1 by the dimensions of the associated elements and their enclosures. Of the two external coaxial circuit ports evident in the photograph, the one linked to the gain section represents the regular intermediate-frequency output port, while the other serves as auxiliary test port. The auxiliary port was used in pre-testing device operation. As it does not otherwise interfere with normal operation, it has not been accounted for in the circuit diagram of Fig. 2.

The front-end section consists of an Avantek M121 sub-quarter-micron GaAs FET embedded in feedback and impedance-matching circuitry. The basic configuration is that of a common-source oscillator, although most any oscillator configuration could be adapted for the present purposes. A lumped-element air inductor in the form of a short piece of bondwire provides drain-to-gate feedback. It serves, in conjunction with transistor gate and drain matching networks, to

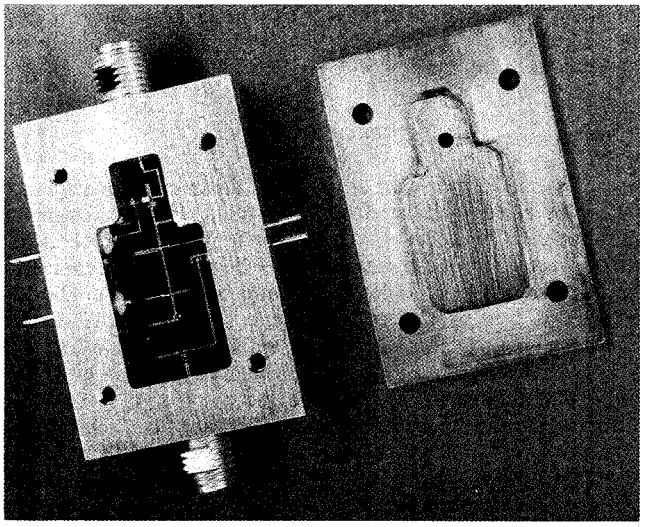

Fig. 1 — Optical demodulator and self-oscillating downconverter, using one single-gate sub-quarter-micron GaAs FET. A second transistor is employed as an intermedidate-frequency buffer amplifier.

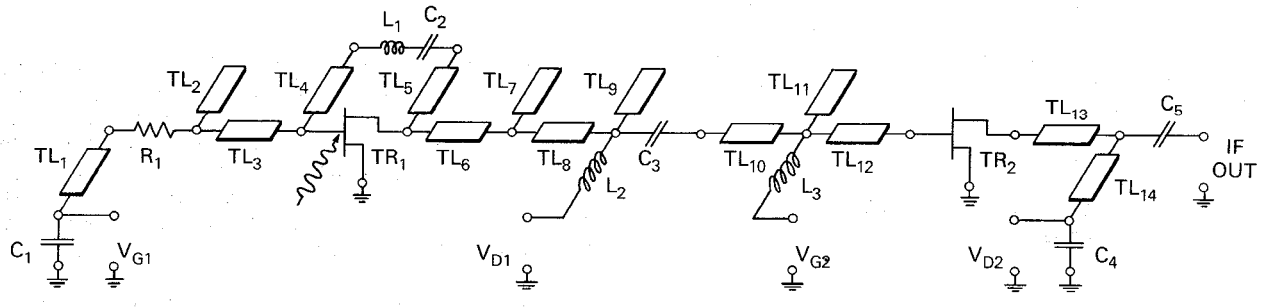

Fig. 2 — Schematic circuit diagram of optical demodulator-downconverter.

establish local oscillation in the vicinity of 30 GHz. The associated circuit resonance is not particularly high-Q, so that the observed oscillating frequency can be tuned by adjusting the bias voltages. The local oscillator signal interacts with the modulated optical carrier signal in the manner discussed previously. The circuit is designed to confine the oscillation signal to the front-end section, while providing a broadband impedance match to the input of the gain stage over the designated intermediate-frequency band centered around 5 GHz. As for the output gain section, it incorporates an Avantek M126 GaAs FET and serves to amplify the intermediate-frequency signal by approximately 9 dB and to provide isolation from external load conditions.

EXPERIMENTAL PERFORMANCE CHARACTERISTICS

The operation of the demodulator-downconverter circuit was tested using the experimental set-up in Fig. 3. To produce the high-frequency intensity-modulated optical carrier, the outputs of two GaAlAs laser diodes operating at 830 nm are combined with the help of a beamsplitter. Varying current and temperature of each diode allows the individual laser frequencies to be offset so as to achieve optical carrier modulation at the desired beat frequency. This difference frequency is observed on a Fabry-Perot interferometer. To decrease the optical linewidth of the associated beat signal, optical feedback is introduced by placing partial reflectors at a distance of 30 cm from each laser. This resulted in a measured beat signal linewidth of 6 MHz.

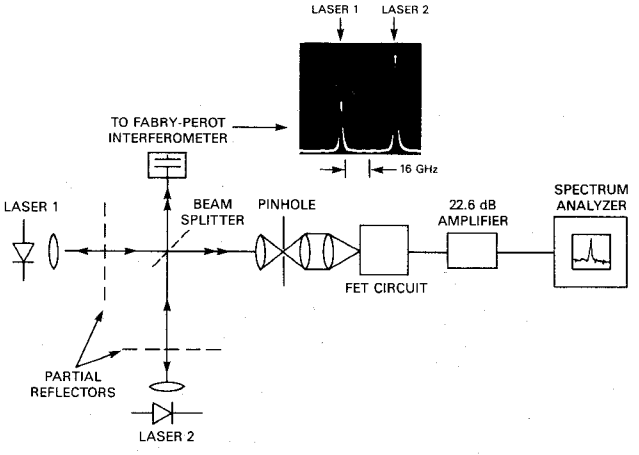

Fig. 3 — Experimental arrangement for optical evaluation of demodulator-downconverter performance.

The combined laser output signals are focused on the unmetallized regions between the source and the drain of the FET. The total available optical power incident on the transistor, taking into account attenuation through the focusing lenses, amounts to −7.2 dBm. The individual contributions to the total power by each of the two laser diodes are 30 percent and 70 percent, respectively. The efficiency of coupling the focused optical beam into the device active area is estimated to be 30 percent.

As previously mentioned, it is assumed in this context that the optical signal levels are small compared to the local oscillator signal amplitude. The validity of the assumption is confirmed by the measurement results displayed in Fig. 4. The measurements are based on an optical carrier modulation frequency of 22.5 GHz, with the transistor biased at a drain-source voltage of +2.0 V and a gate-source voltage of −1.0 V relative to a pinch-off voltage of approximately −2.5 V. The observed quadratic dependence of intermediate-frequency output power on incident optical power conforms with expectations for small-signal operation. The dependence reflects proportionality between optical power and optically-induced current. The minor deviations of experimental points from the idealized curve correspond to the experienced measurement accuracy of about 1 dB.

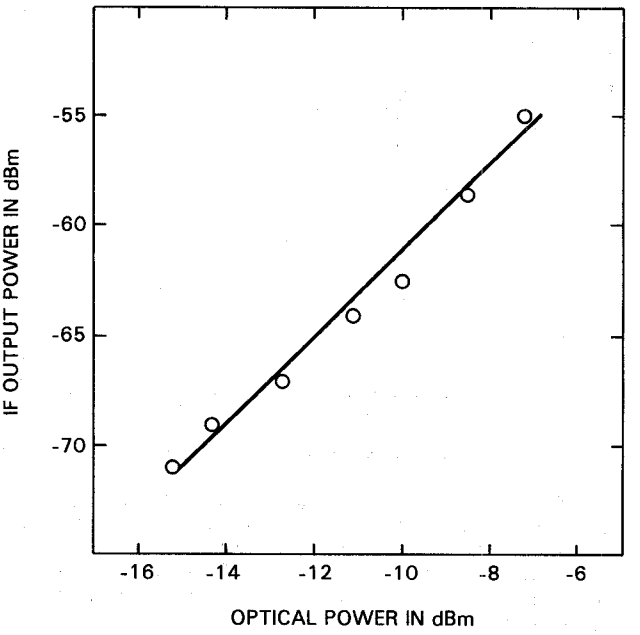

Fig. 4 — Measured intermediate-frequency output power at 5 GHz as a function of total incident optical power with a modulation frequency of 22.5 GHz. The drain-source and gate-source bias voltages for the front-end transistor are $V_{ds} = +2.0\ V$ and $V_{gs} = -1.0\ V$, respectively.

To gain some insight into actual circuit operation, intermediate-frequency output power has been measured as a function of gate-source bias voltage. Figure 5 depicts the measured responses for signal interaction involving the internally generated local oscillator signal at frequency f_{lo}, its second and third harmonics, and the optical carrier with superimposed modulation at frequency f_m. At a given intermediate frequency f_{if}, each harmonic yields both a lower sideband and an upper sideband response for associated modulation frequencies $f_m = nf_{lo} \pm f_{if}$, where $n = 1, 2, 3, \ldots$. In the measurement, the frequency of the generated output signal was kept constant at 6.5 GHz. As the local oscillator frequency changes with bias voltage, it was hence necessary to retune the optical carrier modulation frequency for each value of gate-source bias voltage. The largest intermediate-frequency response of −55 dBm occurred at

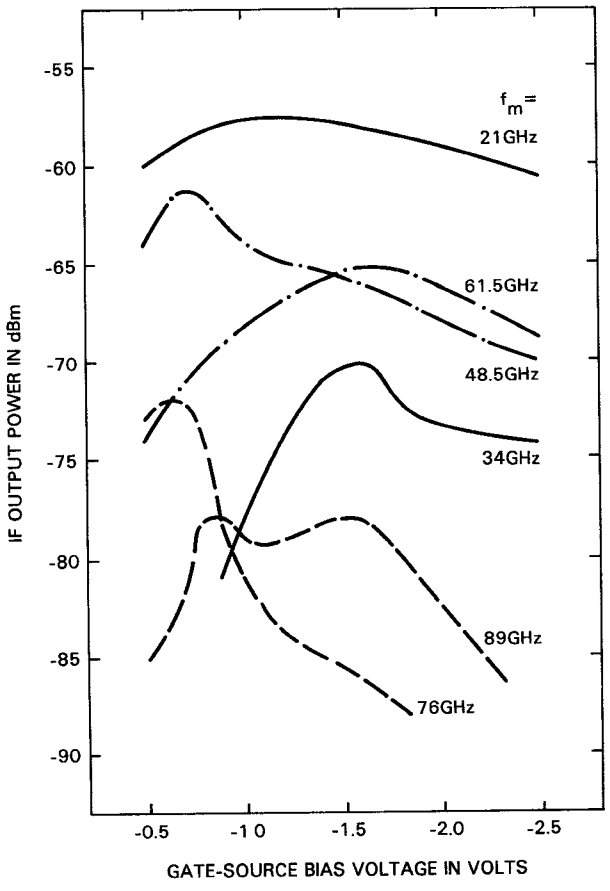

Fig. 5 — Measured output responses for a fixed intermediate frequency of 6.5 GHz plotted as function of gate-source bias voltage applied to the front-end transistor. The parameter f_m designates the optical carrier modulation frequency associated with each curve for the particular gate-source bias voltage of $V_{gs} = -1.0V$.

a modulation frequency of f_m = 22.5 GHz. After amplification (Fig. 3), the signal displayed on the spectrum analyzer was 35 dB above the noise floor.

The demodulation and downconversion characteristics shown in Fig. 5 are a reflection of the complex, multifunctional task assigned to the transistor. In addition to the different signal interaction modes discussed earlier, the embedding network exerts a significant influence on overall circuit performance, which leads to constructive or destructive signal interaction, depending on the particular circumstances. Unfortunately, circuit performance as a function of external bias voltage tends to be obscured by signal clamping and gate biasing effects internal to the transistor, such as have been observed in the related case of a self-oscillating frequency multiplier [8]. Nevertheless, each individual response curve in Fig. 5 displays its own characteristic dependence on bias voltage, indicating differences in the way the composite demodulation and downconversion process is accomplished in each situation. The device-external network plays a decisive role in establishing these differences. The embedding network is thereby primarily designed to optimize local oscillator characteristics and impedance matching conditions in the intermediate-frequency band. No specific steps were taken to address the optimization of circuit conditions at the various sideband frequencies, as the underlying objective was mainly to explore viability of the basic concept. Experimental results, indeed, confirm the practicability of the investigated composite demodulator and downconverter approach, while simultaneously providing an estimate for achievable performance characteristics.

CONCLUSIONS

The concept investigated here relies on one single-gate GaAs FET to perform the multifunctional task of demodulating a high-frequency modulated optical carrier, of downconverting the modulation signal to a lower frequency band, of internally generating a local oscillator signal, and of producing harmonics thereof for use in harmonic downconversion. The circuit exhibits performance competitive with diode-based alternatives for optical carrier modulation frequencies extending up into the 90 GHz range. Among the attractive features of the transistor circuit are its simplicity, its compact physical realization, and the fact that it relies solely on commercially available components.

REFERENCES

1. J. E. Bowers, et al., "High-frequency constricted mesa lasers," Appl. Phys. Lett., vol. 47, pp. 78-80, 1985.
2. R. S. Tucker, "High-speed modulation of semiconductor lasers," IEEE Trans. Electron Dev., vol. ED-32, pp. 2572-2584, 1985.
3. L. Goldberg, et al., "35 GHz microwave signal generation with an injection locked laser diode," Electron. Lett., vol. 21, pp. 814-816, 1985.
4. D. K. Donald, et al., "Efficient simple optical heterodyne receiver: DC to 80 GHz," presented at 1985 SPIE Conf., Washington, DC.
5. H. Mizuno, "Microwave characteristics of an optically controlled GaAs MESFET," IEEE Trans. Microwave Theory Tech., vol. MTT-31, pp. 596-600, 1983.
6. J. C. Gammel and J. M. Ballantyne, "The OPFET: A new high speed optical detector," in Proc. IEDM, 1978, pp. 120-123.
7. C. Rauscher and H. A. Willing, "Simulation of nonlinear microwave FET performance using a quasi-static model," IEEE Trans. Microwave Theory Tech., vol. MTT-27, pp. 834-840, 1979.
8. C. Rauscher, "High-frequency doubler operation of GaAs field-effect transistors," IEEE Trans. Microwave Theory Tech., vol. MTT-31, pp. 555-564, 1982.